APPLIED AND ENVIRONMENTAL MICROBIOLOGY, Jan. 1996, p. 13–19 Vol. 62, No. 1
0099-2240/96/$04.00+0

Degradation of Pyrene, Benz[*a*]anthracene, and Benzo[*a*]pyrene by *Mycobacterium* sp. Strain RJGII-135, Isolated from a Former Coal Gasification Site

JOANNE SCHNEIDER,[1] ROBERT GROSSER,[2] KOKA JAYASIMHULU,[1] WEILING XUE,[1] AND DAVID WARSHAWSKY[1]*

Department of Environmental Health, University of Cincinnati, Cincinnati, Ohio 45267-0056,[1] and Department of Biological Sciences, University of Cincinnati, Cincinnati, Ohio 45221-0006[2]

Received 2 June 1995/Accepted 10 October 1995

The degradation of three polycyclic aromatic hydrocarbons (PAH), pyrene (PYR), benz[*a*]anthracene (BAA), and benzo[*a*]pyrene (BaP), by *Mycobacterium* sp. strain RJGII-135 was studied. The bacterium was isolated from an abandoned coal gasification site soil by analog enrichment techniques and found to mineralize [^{14}C]PYR. Further degradation studies with PYR showed three metabolites formed by *Mycobacterium* sp. strain RJGII-135, including 4,5-phenanthrene-dicarboxylic acid not previously isolated, 4-phenanthrene-carboxylic acid, and 4,5-pyrene-dihydrodiol. At least two dihydrodiols, 5,6-BAA-dihydrodiol and 10,11-BAA-dihydrodiol, were confirmed by high-resolution mass spectral and fluorescence analyses as products of the biodegradation of BAA by *Mycobacterium* sp. strain RJGII-135. Additionally, a cleavage product of BAA was also isolated. Mass spectra and fluorescence data support two different routes for the degradation of BaP by *Mycobacterium* sp. strain RJGII-135. The 7,8-BaP-dihydrodiol and three cleavage products of BaP, including 4,5-chrysene-dicarboxylic acid and a dihydro-pyrene-carboxylic acid metabolite, have been isolated and identified as degradation products formed by *Mycobacterium* sp. strain RJGII-135. These latter results represent the first example of the isolation of BaP ring fission products formed by a bacterial isolate. We propose that while this bacterium appears to attack only one site of the PYR molecule, it is capable of degrading different sites of the BAA and BaP molecules, and although the sites of attack may be different, the ability of this bacterium to degrade these PAH is well supported. The proposed pathways for biodegradation of these compounds by this *Mycobacterium* sp. strain RJGII-135 support the dioxygenase enzymatic processes reported previously for other bacteria. Microorganisms like *Mycobacterium* sp. strain RJGII-135 will be invaluable in attaining the goal of remediation of sites containing mixtures of these PAH.

The presence of polycyclic aromatic hydrocarbons (PAH) in contaminated soils continues to pose significant problems. Levels of these compounds vary from 5 ppb for an undeveloped area of Alaska to 1.79×10^6 ppb for an oil refinery outfall in Southampton, England (12). Their hydrophobicity is cited as the primary reason for their persistence in soils and sediments. This is especially true for larger PAH such as pyrene (PYR), benz[*a*]anthracene (BAA), and benzo[*a*]pyrene (BaP), which have very low water solubilities (0.140 mg of PYR liter^{-1}; 0.002 mg of BAA liter^{-1}; 0.003 mg of BaP liter^{-1}) (19). Their prevalence in contaminated soil at hazardous waste sites are 1,808 ppb for PYR, 2,320 ppb for BAA, and 3,101 ppb for BaP compared with 1 to 19.7 ppb for PYR, 5 to 20 ppb for BAA, and 2 to 1,300 ppb for BaP in rural soils (19). While PYR is not considered a carcinogen, it is prevalent in contaminated soils (71% of sites tested) (19) and is mutagenic as determined by the Ames assay (9). Both BaP and BAA are commonly found in contaminated soils (47% sites contain BaP, and 41% contain BAA) (19), and BaP is considered a potent carcinogen, while BAA is considered a moderate to weak carcinogen (10).

Of the processes whereby these contaminants such as PYR, BAA, and BaP are removed from the environment, microbial degradation plays a major role in the decontamination of sediment and surface soils (17). With the aim of remediation and removal of these compounds from the environment, it is essential to understand the pathways of degradation for those compounds which are found at these sites. While two- to three-ring PAH degradation by microorganisms is well understood and documented (see reference 4 for a review), the microbial biodegradation of the larger-ring PAH has not been studied extensively. Of the three molecules PYR, BAA, and BaP, PYR degradation has been studied to the greatest extent, and the degradation of four-ring compounds such as PYR and fluoranthene is well documented (3, 4, 7, 8, 13).

While BaP degradation has been reported (5), only the *cis*-9,10-BaP-dihydrodiol and 7,8-BaP-dihydrodiol formed by *Beijerinckia* sp. (5) have been identified as intermediates; no ring cleavage products have been isolated. Isolated intermediates of BAA degradation by *Beijerinckia* sp. strain B1 have included three dihydrodiols, namely, *cis*-1,2-BAA-dihydrodiol, *cis*-8,9-BAA-dihydrodiol, and *cis*-10,11-BAA-dihydrodiol (5, 11), as well as ring cleavage products 1-hydroxy-2-anthracene-carboxylic acid, 2-hydroxy-3-phenanthrene-carboxylic acid, and 3-hydroxy-2-phenanthrene-carboxylic acid (15). As part of our overall aim to enhance microbial biodegradation of PAH, we present proposed pathways of PYR, BAA, and BaP degradation by *Mycobacterium* sp. strain RJGII-135 which include the formation of dihydrodiols and ring fission intermediates.

MATERIALS AND METHODS

Chemicals. All solvents used were high-performance liquid chromatography (HPLC) or Optima grade and obtained from Fisher Scientific (Pittsburgh, Pa.). [4,5,9,10-^{14}C]PYR with a specific activity of 59.5 mCi mmol^{-1} was purchased from Chemsyn Science Laboratories (Lenexa, Kans.). [7,10-^{14}C]BaP with a spe-

* Corresponding author. Mailing address: Department of Environmental Health, University of Cincinnati, P.O. Box 670056, Cincinnati, OH 45267-0056. Phone: (513) 558-0152. Fax: (513) 558-5561.

TABLE 1. High-resolution mass spectral data of PYR metabolites formed by *Mycobacterium* sp. strain RJGII-135

Metabolite	Molecular ion observed mass (expected)	Relative intensity	Elemental analysis	Characteristics of major fragments[a]
PYR-I (methylated-4-phenanthrene-carboxylic acid)	236.0821 (236.0837)	100	$C_{16}H_{12}O_2$	205.0644, 53, $C_{15}H_9O$; 177.0716, 38, $C_{14}H_9$
PYR-II (methylated-4,5-phenanthrene dicarboxylic acid)	294.0891 (294.0892)	7	$C_{18}H_{14}O_4$	235.0767, 100, $C_{16}H_{11}O_2$; 220.0558, 35, $C_{15}H_8O_2$
PYR-III (4,5-pyrene-dihydrodiol)	236.0819 (236.0837)	59	$C_{16}H_{12}O_2$	218.0691, 100, $C_{16}H_{10}O$; 202.0832, 13, $C_{16}H_{10}$; 189.0709, 50, $C_{15}H_9$

[a] Characteristics for each fragment are listed in order of mass, relative intensity, and elemental analysis data.

cific activity of 59.2 mCi $mmol^{-1}$ and [12-^{14}C]BAA with a specific activity of 48.3 mCi $mmol^{-1}$ were purchased from Amersham (Arlington Heights, Ill.). Nonradiolabeled PYR, BAA, BaP, and chrysene were purchased from Aldrich (Milwaukee, Wis.). Authentic *trans*-10,11-dihydrodiol-benz[*a*]anthracene, *cis*-5,6-dihydro-5,6-dihydroxy-benz[*a*]anthracene, *trans*-8,9-dihydro-8,9-dihydroxy-benz[*a*]anthracene, and *cis*-7,8-dihydro-7,8-dihydroxy-benzo[*a*]pyrene standards were purchased from NCI Chemical Carcinogen Repository at Midwest Research Institute (Kansas City, Mo.). PYR, BAA, BaP, and chrysene were further purified by neutral alumina column chromatography, elution by toluene, and recrystallization with benzene-isopropanol. The purity of all of these compounds was checked by HPLC and found to be >99%. All experiments, manipulations, and analyses were performed under gold light to prevent photooxidation (Armalite diffuser shields [Thermoplastics, Sterling, N.J.] and Rosculux [Rosco, Port Chester, N.Y.]).

Bacterial growth conditions. The *Mycobacterium* sp. strain RJGII-135 was isolated from a former coal gasification site soil by analog enrichment (6). The methods used for continual growth and maintenance of the bacterium have been reported previously (6). Briefly, the *Mycobacterium* sp. strain RJGII-135 cells were maintained in minimal basal salts medium (MBS) (18) with 0.5 μg of PYR ml^{-1} and 250 μg each of yeast extract, peptone, and soluble starch ml^{-1}.

Metabolism studies. Pure cultures of the bacterial isolate were used to study degradation patterns of [^{14}C]PYR by serum bottle radiorespirometry (14). Time course studies were accomplished with cultures containing 10 ml of MBS and 5 μg of PYR (0.5 μCi of [^{14}C]PYR). At each time point (0, 0.5, 1, 2, 4, and 8 h), wicks containing $^{14}CO_2$ were removed and diluted with Scintiverse BD scintillation cocktail (Fisher Scientific), and ^{14}C radioactivity was quantified with a Packard (Downers Grove, Ill.) Tri-Carb model 2200CA scintillation counter. The cultures were then centrifuged, and the growth medium was extracted twice with ethyl acetate (1:1, vol/vol). The organic layers were pooled and dried completely under nitrogen (N_2) for HPLC analyses.

Pure cultures of the bacterial isolate were also used to study the degradation patterns of [^{14}C]BAA and [^{14}C]BaP. Time course studies were accomplished with *Mycobacterium* sp. strain RJGII-135 cultures containing 50 ml of MBS and 20 μg of BAA or BaP (0.5 μCi of [^{14}C]BAA or 0.5 μCi of [^{14}C]BaP). At the time points (1, 2, 4, 8, 16, and 32 days), the cultures were extracted twice with ethyl acetate (1:1, vol/vol), dried, and frozen for HPLC analysis as described above.

Analysis and identification of metabolites. Analysis of the metabolites of PYR, BaP, and BAA formed by *Mycobacterium* sp. strain RJGII-135 required cultures containing 1,200 ml of MBS, *Mycobacterium* sp. strain RJGII-135, one of the nonradiolabeled PAH (900 to 1,000 μg of PYR, BAA, or BaP), and cofactors as described above. After 2 weeks of growth, these cultures were centrifuged to remove cells and then extracted twice with ethyl acetate (1:0.5, vol/vol). The ethyl acetate layers were evaporated to partial dryness with a rotary evaporator and then dried completely under N_2 for HPLC analyses.

HPLC analyses. Reversed-phase HPLC analyses were performed with a Waters liquid chromatographic system (Millipore Corp., Milford, Mass.) containing two model 501 solvent pumps, a Waters U6K manual injector, a Waters system interface module controller, and a Waters 484 absorbance detector, all controlled by Waters Maxima 820 chromatographic software. All analyses utilized a Whatman Partisil-10, octadecyl silane-2, 10-μm (25 by 0.46 cm [inside diameter]) column, a linear methanol-water gradient (50 to 100% methanol in 30 min), and a flow rate of 1 ml min^{-1}. Dried organic extracts from the radiolabeled and nonradiolabeled experiment cultures were redissolved in 150 to 250 μl of chloroform, and injections of 10 to 15 μl were made onto the HPLC column. The UV A_{254} of the eluate was monitored for all injections. One-minute fractions were collected from injections of the ^{14}C-labeled extracts and diluted with 5 ml of Scintiverse I (Fisher Scientific), and the ^{14}C radioactivity was quantified with a Packard Tri-Carb 460 scintillation counter. Fractions corresponding to UV-absorbing peaks from the nonradiolabeled experiment cultures were also collected.

Fluorescence-mass spectral analyses. Fractions from repeated injections of the nonradiolabeled experiments were pooled and evaporated to dryness under N_2. These metabolites as well as the authentic standards were redissolved in methanol, and standard emission and excitation fluorescence spectra were obtained with a Perkin-Elmer (Norwalk, Conn.) model MPF66 fluorescent spectrophotometer with a series 7700 computer. These bacterial metabolites were then derivatized by methylation with gaseous diazomethane (9) or silylation with *N*,*O*-bis-(trimethylsilyl)-trifluoroacetamide plus 1% trimethylchlorosilane (BSTFA–1% TMCS) (1) prior to mass spectral analyses. A Kratos MS 80 mass spectrometer was used to obtain high-resolution (resolution is 3,000) mass spectral data of the derivatives of the isolated metabolites with an internal standard of perfluorokerosene. The samples were introduced into the mass spectrometer either by direct insertion probe or on column injection onto a Carbo Erba gas chromatograph interfaced with the mass spectrometer.

RESULTS

Kinetics of PYR degradation and metabolite formation. A kinetic experiment was conducted to determine the time course for PYR degradation and the formation of specific PYR metabolites by *Mycobacterium* sp. strain RJGII-135 cultures. The degradation of [^{14}C]PYR was monitored, by HPLC, for up to 8 h. After 8 h of incubation, most of the [^{14}C]PYR was degraded to metabolites by bacterial cultures; degradation did not occur in the sterile controls. Four metabolite fractions of PYR, designated PYR-I, PYR-II, PYR-III, and PYR-IV, were detected by HPLC-UV and radioactivity-HPLC elution profiles of organic extracts with retention times of 5.4, 6.8, 21.1, and 29.0 min, respectively (undegraded PYR retention time, 39 min).

Over 40% of the [^{14}C]PYR was mineralized to $^{14}CO_2$ by *Mycobacterium* sp. strain RJGII-135 during the first 2 h of incubation, with greater than 45% mineralization of [^{14}C]PYR by 4 h. Undegraded PYR accounted for 22.5% of the organic-extractable residue during the first 0.5 h of incubation and for 9.5% by 4 h. During the same time period, there were increases of the four metabolites, and by 4 h, metabolites PYR-I, PYR-II, PYR-III, and PYR-IV accounted for 18.6, 21.2, 0.6, and 38.7% of the total organic extractable residues. At 8 h, the values did not change significantly for mineralization nor for metabolite formation, suggesting nutrient depletion.

PYR metabolite identification. The *Mycobacterium* sp. strain RJGII-135 was incubated with nonradiolabeled PYR for 2 weeks; HPLC analysis of the organic extract of the growth medium showed four intermediates of degradation, which were identified. Of the four metabolites, PYR-I, PYR-II, and PYR-III, after methylation, gave mass spectral data and elemental compositions for the molecular ion ($M^{+\cdot}$) and major fragment patterns (Table 1). Metabolite PYR-I at an HPLC retention time of 5.4 min gave a $M^{+\cdot}$ at *m/z* 236 with an elemental analysis of $C_{16}H_{12}O_2$ and fragment ions at *m/z* 205 with elemental analysis of $C_{15}H_9O$ ($M^{+\cdot} - 31$, CH_3O loss) and 177 with an elemental analysis of $C_{14}H_9$ ($M^{+\cdot} - 59$, CO_2CH_3 loss). The mass spectral data are consistent with the structure of 4-phenanthrene-carboxylic acid formed by *Mycobacterium* sp. strain PYR-1 (8).

Metabolite PYR-II at an HPLC retention time of 6.8 min

TABLE 2. Percent radioactivity in BAA metabolites formed by *Mycobacterium* sp. strain RJGII-135 after incubation with [^{14}C]BAA

Metabolite	% Radioactivity on day:							
	0	1	2	3	4	8	16	32
BAA-I	0	1	1	3	2	4	9	7
BAA-II	0	1	1	2	1	3	5	6
BAA-III	0	4	3	4	2	4	7	5
BAA-IV	0	2	2	4	3	5	9	7
BAA-V	1	12	16	16	20	30	18	25
BAA	97	75	68	60	61	37	26	12

gave a $M^{+\cdot}$ ion at *m/z* 294 with an elemental analysis of $C_{18}H_{14}O_4$, a base peak at *m/z* 235 with an elemental analysis of $C_{16}H_{11}O_2$ ($M^{+\cdot}$ −59, CO_2CH_3 loss), and a fragment ion at *m/z* 220 with elemental analysis of $C_{15}H_8O_2$ ($M^{+\cdot}$ −74, CH_3 and CO_2CH_3 loss) (Table 1). The mass spectral analysis is consistent with the assignment 4,5-phenanthrene-dicarboxylic acid. This metabolite has not been isolated previously (8), although it has been suggested as a stable intermediate in the microbial degradation pathway of PYR by *Mycobacterium* sp. strain PYR-1 (4).

Metabolite PYR-III at an HPLC retention time of 21.1 min was the PYR major metabolite produced by *Mycobacterium* sp. strain RJGII-135. This metabolite had a $M^{+\cdot}$ at *m/z* 236 with an elemental analysis of $C_{16}H_{12}O_2$, a base peak of 218, and an elemental analysis of $C_{16}H_{10}O$ ($M^{+\cdot}$ −18, H_2O loss) and fragment ions at *m/z* 202 with an elemental analysis of $C_{16}H_{10}$ ($M^{+\cdot}$ −34, two OH loss) and at *m/z* 189 with an elemental analysis of $C_{15}H_9$ ($M^{+\cdot}$ −47, COH and H_2O loss) (Table 1). Fluorescence spectra of this metabolite shows a phenanthrene structure indicating that either aromatic ring two or four of PYR is saturated, which would be consistent with a pyrene-dihydrodiol structure. On the basis of mass spectral and fluorescence data, metabolite PYR-III is identified as 4,5-pyrene-dihydrodiol, which is consistent with the assigned structure reported by Heitkamp et al. for *Mycobacterium* sp. strain PYR-1 (8).

Kinetics of BAA degradation and metabolite formation. Studies with *Mycobacterium* sp. strain RJGII-135 and [12-^{14}C]BAA showed the formation of at least five metabolites, designated BAA-I, BAA-II, BAA-III, BAA-IV, and BAA-V, with retention times of 24, 26.4, 28.2, 31, and 34 min, respectively (undegraded BAA retention time, 40 min). The degradation of [^{14}C]BAA was concommitant with the increase in these metabolites over 32 days (Table 2). Sterile controls showed no degradation. The degradation by *Mycobacterium* sp. strain RJGII-135 was fairly rapid since metabolite BAA-V, with an HPLC retention time of 35 min, was present at 11% after only 1 day. Following 8 days of incubation, only ~36% of the original [^{14}C]BAA remained, while metabolite BAA-V had increased to ~30%. Undegraded BAA accounted for 11% of the organic-extractable residue, and the other metabolites accounted for >48% of the radioactivity at 32 days, clearly demonstrating degradation of BAA by *Mycobacterium* sp. strain RJGII-135.

BAA metabolite identification. To accurately identify the degradation products of BAA, *Mycobacterium* sp. strain RJGII-135 was incubated with nonradiolabeled BAA for 2 weeks. This time point appeared to be optimal for obtaining sufficient quantities of all metabolites. Organic extracts of growth medium were injected onto the HPLC and analyzed by mass spectral and fluorescence analyses.

HPLC peak BAA-II, at 26.4 min, cochromatographed with the standard *cis*-5,6-BAA-dihydrodiol. Trimethylsilylated metabolite BAA-II gave a $M^{+\cdot}$ at *m/z* 406 with an elemental composition of $C_{24}H_{30}O_2Si_2$ and fragment ions at *m/z* 334 with an elemental analysis of $C_{21}H_{22}O_2Si$ ($M^{+\cdot}$ −72, C_3H_8Si loss) and at *m/z* 316 with an elemental analysis of $C_{21}H_{20}OSi$ ($M^{+\cdot}$ −90, $C_3H_{10}OSi$ loss) (Table 3). The mass spectral data of trimethylsilylated metabolite BAA-II are consistent with trimethylsilylation of standard *cis*-5,6-BAA-dihydrodiol. Additionally, the fluorescence spectra of metabolite BAA-II are coincident with the fluorescence spectra of authentic standard *cis*-5,6-BAA-dihydrodiol (Fig. 1A). On the basis of these data, metabolite BAA-II is assigned the structure *cis*-5,6-BAA-dihydrodiol.

Metabolite BAA-III was the major BAA metabolite formed by *Mycobacterium* sp. strain RJGII-135. Trimethylsilylated metabolite BAA-III gave a $M^{+\cdot}$ at *m/z* 406 with an elemental composition of $C_{24}H_{30}O_2Si_2$ and fragment ions at *m/z* 334 with an elemental analysis of $C_{21}H_{22}O_2Si$ ($M^{+\cdot}$ −72, C_3H_8Si loss) and at *m/z* 316 with an elemental analysis of $C_{21}H_{20}OSi$ ($M^{+\cdot}$ −90, $C_3H_{10}OSi$ loss) (Table 3). These mass spectral data are consistent with those of the trimethylsilylated standard *trans*-10,11-BAA-dihydrodiol. Additionally, the fluorescence spectra of metabolite BAA-III match the fluorescence spectra of the authentic *trans*-10,11-BAA-dihydrodiol (Fig. 1B). HPLC peak BAA-III at 28 min chromatographed closely with the *trans*-10,11-BAA-dihydrodiol; the *cis* isomer is not available for comparison. On the basis of these data and since formation of *trans* isomers by bacteria is rare (4), metabolite BAA-III is assigned the structure of *cis*-10,11-BAA-dihydrodiol.

Another metabolite, BAA-I, present at 24 min on the HPLC, may be *cis*-8,9-BAA-dihydrodiol, although the metabolite fluorescence spectra are shifted by 5 to 7 nm from that seen for the *trans*-8,9-BAA-dihydrodiol standard (data not shown). The *trans*-8,9-BAA-dihydrodiol standard elutes on HPLC at 28 min, almost 4 min after this metabolite; the *cis* isomer is not available. These differences in HPLC elution patterns could be due to differences between the *trans* and *cis* isomers. Since this metabolite appears in very small quantities, a good mass spectral analysis has not been obtained; the confirmation of this metabolite awaits further experimentation. The mass spectra of another metabolite (BAA-IV) at an

TABLE 3. High-resolution mass spectral data of BAA metabolites formed by *Mycobacterium* sp. strain RJGII-135

Metabolite	Molecular ion observed mass (expected)	Relative intensity	Elemental analysis	Characteristics of major fragments[a]
BAA-II (*cis*-5,6-BAA-trimethylsilylated dihydrodiol)	406.1773 (406.1784)	72	$C_{24}H_{30}O_2Si_2$	334.1350, 14, $C_{21}H_{22}O_2Si$; 316.1306, 100, $C_{21}H_{20}OSi$
BAA-III (*cis*-10,11-BAA-trimethylsilylated dihydrodiol)	406.1788 (406.1784)	9	$C_{24}H_{30}O_2Si_2$	334.1422, 16, $C_{21}H_{22}O_2Si$; 316.1282, 100, $C_{21}H_{20}OSi$

[a] Characteristics for each fragment are listed in order of mass, relative intensity, and elemental analysis data.

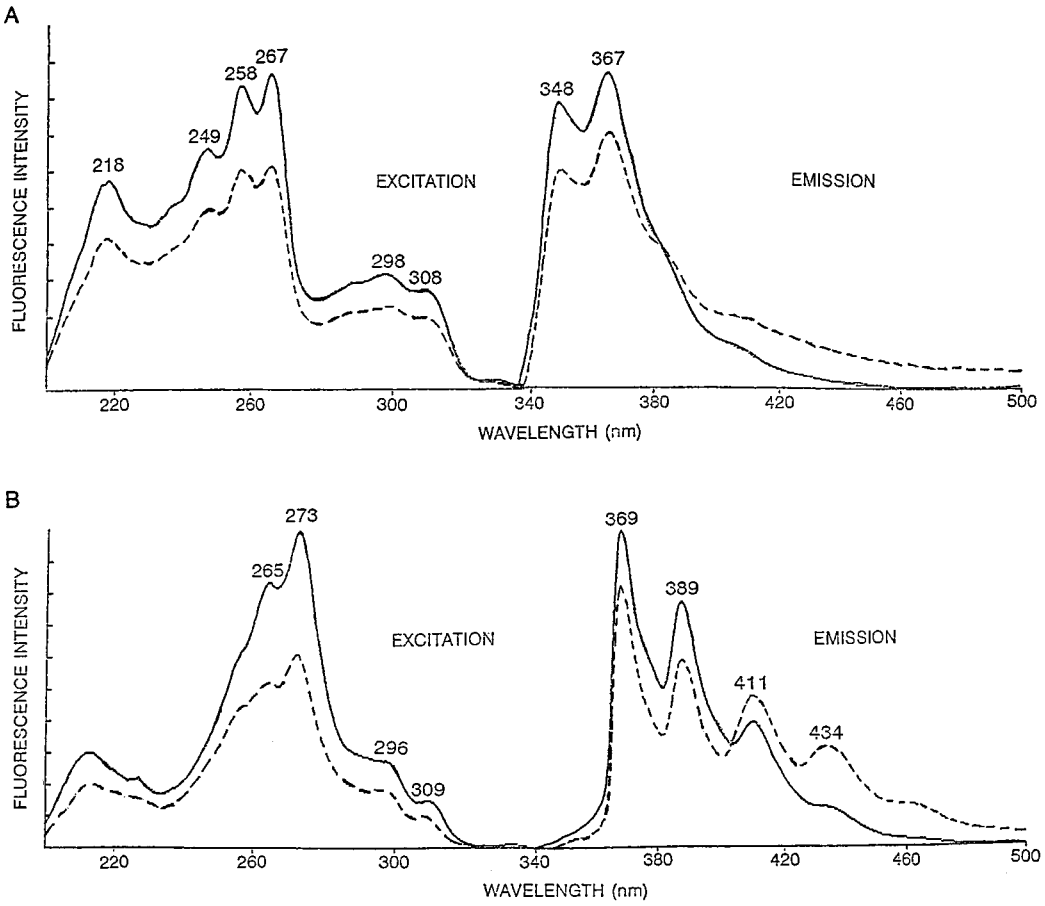

FIG. 1. Fluorescence spectra of *cis*-BAA-5,6-dihydrodiol standard (-) and *Mycobacterium* sp. strain RJGII-135 metabolite BAA-II (--) (A) and *trans*-10,11-dihydrodiol-BAA standard (-) and *Mycobacterium* sp. strain RJGII-135 metabolite BAA-III (--) (B).

HPLC retention time of 31 to 32 min gave a $M^{+\cdot}$ at *m/z* 246.0681 with an elemental analysis of $C_{17}H_{10}O_2$. While a structure has not been assigned to this metabolite, it represents a ring cleavage intermediate of BAA formed by *Mycobacterium* sp. strain RJGII-135.

Kinetics of BaP degradation and metabolite formation. Studies of *Mycobacterium* sp. strain RJGII-135 with [^{14}C]BaP showed the formation of at least six metabolites, designated BaP-I, BaP-II, BaP-III, BaP-IV, BaP-V, and BaP-VI, with retention times of 14, 16, 30, 33, 35, and 36 min, respectively (BaP retention time, 42 min). The kinetics of BaP degradation and metabolite formation by *Mycobacterium* sp. strain RJGII-135 was much slower than that seen for PYR or BAA degradation (Table 4). After 32 days, undegraded [^{14}C]BaP accounted for ~60% of the organic-extractable residue; sterile controls showed no degradation. Similarly, the formation of the metabolites increased slowly from 0 to ~9% over 32 days for metabolites III and V, from 0 to ~6% for metabolite VI, and from 0 to ~2% for metabolite BaP-IV.

BaP metabolite identification. To accurately determine the BaP degradation pathway and metabolite identification, *Mycobacterium* sp. strain RJGII-135 was incubated with nonradiolabeled BaP for 2 weeks. The organic extracts of the growth medium were separated by HPLC and analyzed by mass spectral and fluorescence analyses. Four metabolites, designated BaP-I, BaP-II, BaP-III, and BaP-IV, were identified by high-resolution mass spectrometry and fluorescence spectroscopy.

Metabolite BaP-I, with an HPLC retention time of 14 min, was methylated and gave a $M^{+\cdot}$ at *m/z* 344 and an elemental analysis of $C_{22}H_{16}O_4$, a base peak at *m/z* 285 with an elemental analysis of $C_{20}H_{13}O_2$ ($M^{+\cdot}$ −59, CO_2CH_3 loss), and a fragment ion at *m/z* 270 with an elemental analysis of $C_{19}H_{10}O_2$ ($M^{+\cdot}$ −74, CH_3 and CO_2CH_3 loss) (Table 5). These data indicate that methylation occurred at a carboxyl group and a hydroxyl group rather than two carboxyl groups. Methylation of the latter would yield a fragment ion showing a loss of two methyl carboxylate groups ($M^{+\cdot}$ −118), which was not shown in the mass spectra. The methylation of both carboxyl and hydroxyl groups in similar compounds, with diazomethane, has

TABLE 4. Percent radioactivity in BAP metabolites formed by *Mycobacterium* sp. strain RJGII-135 after incubation with [^{14}C]BAP

Metabolite	% Radioactivity on day:							
	0	1	2	3	4	8	16	32
BAP-I	0	0	0	0	0	1	0	0
BAP-II	0	0	0	0	0	0	0	0
BAP-III	0	2	1	3	2	3	2	10
BAP-IV	0	2	1	2	2	3	3	2
BAP-V	1	3	5	6	7	7	8	9
BAP-VI	2	7	5	4	5	7	10	7
BAP	94	80	85	82	80	70	69	61

TABLE 5. High-resolution mass spectral data of BaP metabolites formed by *Mycobacterium* sp. strain RJGII-135

Metabolite	Molecular ion observed mass (expected)	Relative intensity	Elemental analysis	Characteristics of major fragments[a]
BaP-I [methylated *cis*-4-(8-hydroxypyrene-7-yl)-2-oxobut-3-enoic acid or *cis*-4-(7-hydroxypyren-8-yl)-2-oxobut-3-enoic acid]	344.1092 (344.1049)	14	$C_{22}H_{16}O_4$	285.0935, 100, $C_{20}H_{13}O_2$; 270.0680, 56, $C_{19}H_{10}O_2$
BaP-II (methylated 4,5-chrysene-dicarboxylic acid)	344.1055 (344.1049)	25	$C_{22}H_{16}H_4$	285.0903, 100, $C_{20}H_{13}O_2$; 270.0661, 58, $C_{19}H_{10}O_2$
BaP-III (*cis*-7,8-dihydrodiol-BaP)	286.0984 (286.0994)	28	$C_{20}H_{14}O_2$	268.0883, 100, $C_{20}H_2O$; 239.0858, 38, $C_{19}H_{11}$
BaP-IV (methylated 7,8-dihydro-pyrene-7-carboxylic acid or 7,8-dihydro-pyrene-8-carboxylic acid)	262.0975 (262.0994)	100	$C_{18}H_{14}O_2$	247.0740, 14, $C_{17}H_{11}O_2$; 202.0791, 37, $C_{16}H_{10}$

[a] Characteristics for each fragment are listed in order of mass, relative intensity, and elemental analysis data.

been reported (2). The fluorescence spectra of the nonmethylated fraction indicate that metabolite BaP-I has a PYR structure with wavelength maxima at 235, 261, 275, 336, 365, 373, 396, and 425 nm, which closely match those of a PYR standard. These high-resolution mass spectral and fluorescence spectral analyses are consistent with a PYR derivative. We cannot, however, distinguish between the *meta* fission products through the 7,8 bond or the 9,10 bond of BaP. In the former case, the structural assignment would be consistent with *cis*-4-(7-hydroxypyren-8-yl)-2-oxobut-3-enoic acid; for the latter, it would be the *cis*-4-(8-hydroxypyren-7-yl)-2-oxobut-3-enoic acid. A fission product through the 8,9 bond of BaP would not form a compound which could produce this mass spectra; hence, this possibility can be ruled out.

Metabolite BaP-II with an HPLC retention time of 16 min was methylated prior to mass spectral analysis. This methylated derivative gave a $M^{+\cdot}$ at *m/z* 344 with an elemental analysis of $C_{22}H_{16}O_4$, a base peak at *m/z* 285 with an elemental analysis of $C_{20}H_{13}O_2$ ($M^{+\cdot}$ −59, CO_2CH_3 loss), and a fragment ion at *m/z* 270 with an elemental analysis of $C_{19}H_{10}O_2$ ($M^{+\cdot}$ −74, CH_3 and $COCH_3$ loss) (Table 5). The fluorescence spectra of the nonmethylated fraction indicate that metabolite BaP-II has

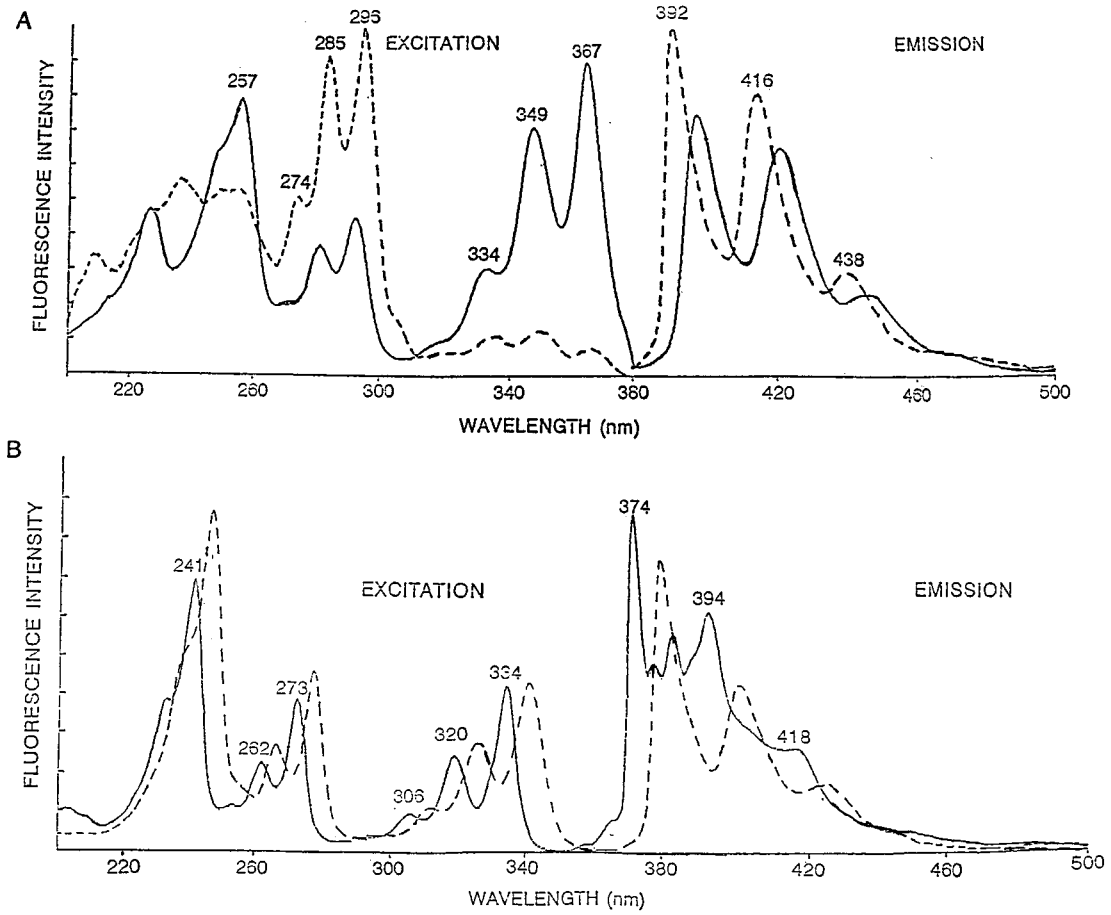

FIG. 2. Fluorescence spectra of *cis*-7,8-BaP-dihydrodiol standard (-) and metabolite BaP-III (--) formed by *Mycobacterium* sp. strain RJGII-135 (A) and PYR standard (-) and metabolite BaP-IV (--) formed by *Mycobacterium* sp. strain RJGII-135 (B).

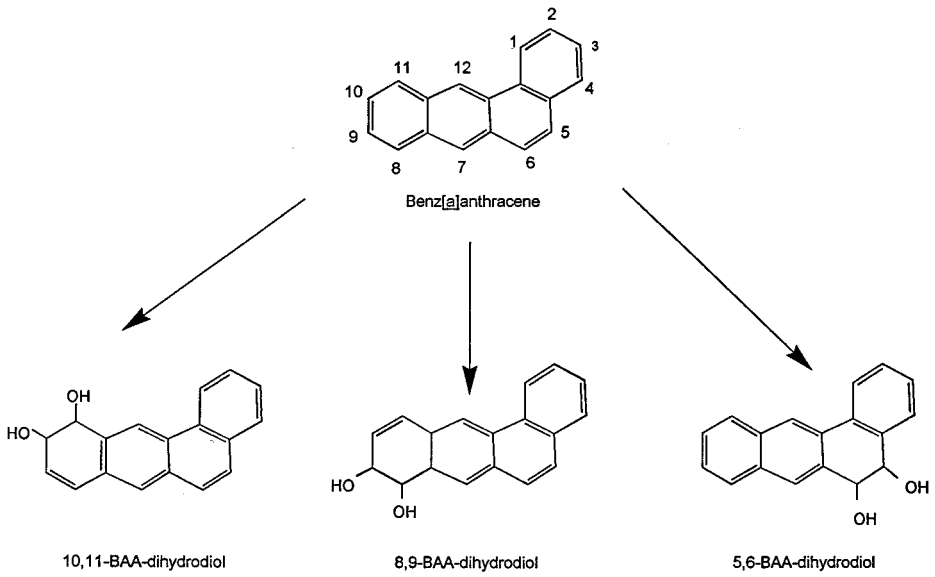

FIG. 3. Proposed pathways for the degradation of BAA by *Mycobacterium* sp. strain RJGII-135 based on isolated metabolites.

a chrysene structure with wavelength maximas of 256, 362, 380, 404, and 428 nm, which are similar to those of an authentic chrysene standard. The mass spectral analysis and fluorescence spectra are consistent with a chrysene dicarboxylic acid derivative, indicating an *ortho* fission product through the 4,5 bond in BaP. Therefore, metabolite BaP-II is assigned the structure of 4,5-chrysene-dicarboxylic acid.

Metabolite BaP-III, which eluted at 30 min on the HPLC, was the major BaP metabolite formed by *Mycobacterium* sp. strain RJGII-135. This metabolite gave a $M^{+\cdot}$ at *m/z* 286 with an elemental analysis of $C_{20}H_{14}O_2$, a base peak at *m/z* 268 with an elemental analysis of $C_{20}H_{12}O$ ($M^{+\cdot}$ −18, H_2O loss), a fragment ion at *m/z* 252 with an elemental analysis of $C_{20}H_{12}$ ($M^{+\cdot}$ −34, two OH loss), and a fragment ion at *m/z* 239 with an elemental analysis of $C_{19}H_{11}$ ($M^{+\cdot}$ −47, COH and H_2O loss). The molecular ion, elemental compositions, and fragment ions are consistent with standard dihydrodiols of BaP. In addition, the HPLC retention time and fluorescence spectra of metabolite BaP-III closely matched those of the authentic standard *cis*-7,8-BaP-dihydrodiol (Fig. 2A). Hence, metabolite BaP-III is assigned the structure *cis*-7,8-BaP-dihydrodiol. Since an authentic 8,9-BaP-dihydrodiol standard is not available for comparison, it is possible that metabolite BaP-III may be the 8,9-dihydrodiol or a mixture of both dihydrodiols.

Metabolite BaP-IV, which eluted at 33 min on the HPLC, was methylated prior to mass spectral analysis. The high-resolution mass spectra of the derivatized metabolite gave a $M^{+\cdot}$ at *m/z* 262 with an elemental analysis of $C_{18}H_{14}O_2$ and fragment ions at *m/z* 247 with an elemental analysis of $C_{17}H_{11}O_2$ ($M^{+\cdot}$ −15, CH_3 loss) and at *m/z* 202 with an elemental analysis of $C_{16}H_{10}$ representing loss of methyl carboxylate (Table 5). The fluorescence spectra of the nonmethylated metabolite BaP-IV is consistent with a PYR structure (Fig. 2B). The shift in fluorescence peak maxima between BaP-IV and PYR is consistent with differences reported between parent compounds and derivatives with aromatic ring saturation and/or substitution (16). The molecular ion, elemental analysis, fragmentation pattern, and fluorescence spectra are consistent with a methylester of dihydro-pyrene-carboxylic acid. As we have indicated for metabolite BaP-I, based on fission of the 7,8-bond and/or the 9,10-bond of BaP, we cannot distinguish between the 7,8-dihydro-pyrene-7-carboxylic acid and 7,8-dihydro-pyrene-8-carboxylic acid structures for this metabolite.

DISCUSSION

We have shown that *Mycobacterium* sp. strain RJGII-135 is capable of mineralizing [^{14}C]PYR to ~50% while producing at least three stable intermediates within a short (4- to 8-h) period of time. These intermediates include the previously reported 4-phenanthrene-carboxylic acid and 4,5-pyrene-dihydrodiol produced by *Mycobacterium* sp. strain PYR-1 (8) and 4,5-phenanthrene-dicarboxylic acid, which had been proposed but not previously isolated from strain PYR-1 (4). The pathway for degradation of PYR by *Mycobacterium* sp. strain RJGII-135 is consistent with that reported for *Mycobacterium* sp. strain PYR-1 (4, 8), which would be expected from members of the same genus.

The formation of at least two different dihydrodiols of BAA by *Mycobacterium* sp. strain RJGII-135 as seen in the proposed pathway (Fig. 3) is similar to previous reports (5, 11, 15) for *Beijerinckia* sp. strain B1, although the 1,2-BAA-dihydrodiol formed preferentially by the *Beijerinckia* sp. was not found in the *Mycobacterium* sp. Unlike the *Beijerinckia* sp., *Mycobacterium* sp. strain RJGII-135 forms 5,6-BAA-dihydrodiol as the predominant metabolite and, secondarily, 10,11-BAA-dihydrodiol. Additionally, the ring cleavage product BAA-IV suggests that this bacterium is capable of cleaving at least one ring of the BAA molecule. The formation of dihydrodiols is consistent with the dioxygenase enzyme pathways proposed for the degradation of other PAH (4), although isolation and identification of the enzymes involved in degradation by this *Mycobacterium* sp. strain RJGII-135 are under investigation.

Before this report, the identified intermediates of microbial BaP degradation were *cis*-9,10-BaP-dihydrodiol and 7,8-BaP-dihydrodiol formed by *Beijerinckia* sp. strain B1 (5). The identification of 7,8-BaP-dihydrodiol formed by this *Mycobacterium* sp. strain RJGII-135 is consistent with those findings. Similarly, we propose that this metabolite is most likely the *cis* isomer. This report of the isolation of three-ring cleavage products of BaP degradation formed from *Mycobacterium* sp. strain RJGII-135 (Fig. 4) is unique. The two pathways for attack of the BaP

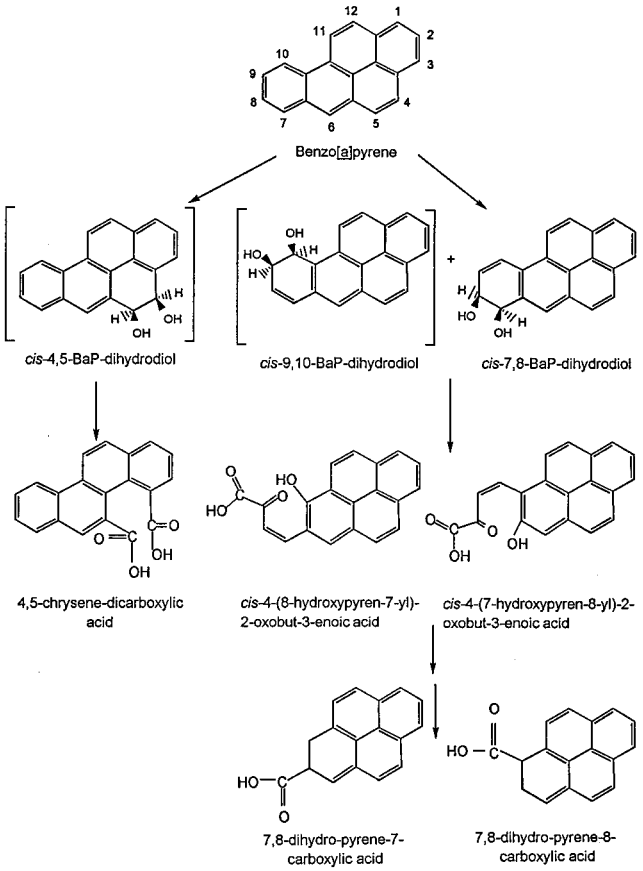

FIG. 4. Proposed pathways for the degradation of BaP by *Mycobacterium* sp. strain RJGII-135 based on isolated metabolites. Structures in brackets are hypothetical intermediates. Arrows between metabolites indicate multiple steps, not single reactions.

molecule by *Mycobacterium* sp. strain RJGII-135 are similar to those proposed for the degradation of BAA by this bacteria and further support the involvement of a dioxygenase enzyme system. Formation of the 4,5-chrysene-dicarboxylic acid intermediate would be consistent with *ortho* fission (4) of the hydroxylated BaP molecule and would be consistent with the $^{14}CO_2$ evolution from [7,10-^{14}C]BaP observed for *Mycobacterium* sp. strain RJGII-135. Formation of *cis*-4-(7-hydroxypyren-8-yl)-2-oxobut-3-enoic acid or *cis*-4-(8-hydroxypyren-7-yl)-2-oxobut-3-enoic acid intermediates from 7,8-BaP-dihydrodiol or 9,10-BaP-dihydrodiol are consistent with *meta* fission (4) of the hydroxylated BaP molecule. Formation of 7,8-pyrene-dihydro-7-carboxylic acid or 7,8-pyrene-dihydro-8-carboxylic acid would involve several steps, as has been proposed for other PAH (15).

In our attempt to biodegrade mixtures of PAH present in coal gasification sites, we have isolated an organism that will allow us to achieve some of our objectives. The *Mycobacterium* sp. strain RJGII-135 appears to degrade both large-ring compounds such as PYR, BAA, and BaP and small-ring compounds such as phenanthrene and anthracene (unpublished data). With a better understanding of the degradation process of PAH by bacteria, strategies will be developed for the removal and containment of carcinogenic PAH from contaminated ecosystems and the reduction of health risks associated with exposure to PAH.

ACKNOWLEDGMENTS

This work was supported by National Institute of Environmental Health Sciences grant P42 ES04908-05.

We thank Leva Wilson for preparing the manuscript.

REFERENCES

1. **Baker, T. S., J. V. Harry, J. W. Russell, and R. L. Myers.** 1984. Rapid method for the GC/MS confirmation of 11-nor-9-carboxy-tetrahydrocannabinol in urine. J. Anal. Toxicol. **8:**255–259.
2. **Black, T. H.** 1983. The preparation and reactions of diazomethane. Aldrichimica Acta **16:**3–10.
3. **Boldrin, B., A. Tiehm, and C. Fritzsche.** 1993. Degradation of phenanthrene, fluorene, fluoranthene, and pyrene by a *Mycobacterium* sp. Appl. Environ. Microbiol. **59:**1927–1930.
4. **Cerniglia, C. E.** 1992. Biodegradation of polycyclic aromatic hydrocarbons. Biodegradation **3:**351–368.
5. **Gibson, D. T., V. Mahadevan, D. M. Jerina, H. Yagi, and H. J. C. Yeh.** 1975. Oxidation of the carcinogens benzo[*a*]pyrene and benz[*a*]anthracene to dihydrodiols by a bacterium. Science **189:**295–297.
6. **Grosser, R. J., D. Warshawsky, and J. R. Vestal.** 1991. Indigenous and enhanced mineralization of pyrene, benzo[*a*]pyrene, and carbazole in soils. Appl. Environ. Microbiol. **57:**3462–3469.
7. **Grosser, R. J., D. Warshawsky, and J. R. Vestal.** 1995. Mineralization of polycyclic and N-heterocyclic aromatic compounds in hydrocarbon-contaminated soils. Environ. Toxicol. Chem. **14:**375–382.
8. **Heitkamp, M. A., J. P. Freeman, D. W. Miller, and C. E. Cerniglia.** 1988. Pyrene degradation by a *Mycobacterium* sp.: identification of ring oxidation and ring fission products. Appl. Environ. Microbiol. **54:**2556–2565.
9. **Holder, C. L., W. A. Korfmacher, W. Slikker, H. C. Thompson, and A. B. Gosnell.** 1985. Mass spectral characterization of doxylamine and its rhesus monkey urinary metabolites. Biomed. Mass. Spectrom. **12:**151–158.
10. **International Agency for Research in Cancer.** 1983. Monograph on the evaluation of carcinogenic risks to humans, vol. 32. International Agency for Research in Cancer, Lyon, France.
11. **Jerina, D. M., D. J. Van Bladeren, H. Yagi, D. T. Gibson, V. Mahadevan, A. S. Neese, M. Koreeda, N. D. Sharma, and D. Boyd.** 1984. Synthesis and absolute configuration of *cis*-1,2-, 8,9- and 10,11-dihydrodiol metabolites of benz[*a*]anthracene formed by a strain of *Beijerinckia* sp. J. Org. Chem. **49:**1075–1082.
12. **Johnson, A. C., and D. Larsen.** 1985. The distribution of polycyclic aromatic hydrocarbons in the surficial sediments of Penobscot Bay (Maine, USA) in relation to possible sources and to other sites worldwide. Mar. Environ. Res. **15:**1.
13. **Kelley, I., J. P. Freeman, F. E. Evans, and C. E. Cerniglia.** 1993. Identification of metabolites from the degradation of fluoranthene by *Mycobacterium* sp. strain PYR-1. Appl. Environ. Microbiol. **59:**800–806.
14. **Knaebel, D. R., and J. R. Vestal.** 1988. A comparison of double vial to serum bottle radiorespirometry to measure microbial mineralization in soils. J. Microbiol. Methods **7:**309–317.
15. **Mahaffey, W. R., D. T. Gibson, and C. C. Cerniglia.** 1988. Bacterial oxidation of chemical carcinogens: formation of polycyclic aromatic acids for benz[*a*]anthracene. Appl. Environ. Microbiol. **54:**2415–2423.
16. **McCaustland, D. J., D. L. Fischer, K. C. Kolwyck, W. P. Duncan, J. C. Wiley, C. S. Menon, J. F. Engel, J. K. Selkirk, and P. P. Roller.** 1976. Polycyclic aromatic hydrocarbon derivatives: synthesis and physiochemical characterization, p. 349–411. *In* R. I. Freudenthal and P. W. Jones (ed.), Polynuclear aromatic hydrocarbons: chemistry, metabolism and carcinogenesis. Raven Press, New York.
17. **Sims, R. C., and M. R. Overcash.** 1983. Fate of polynuclear aromatic compounds (PNAs) in soil-plant system. Residue Rev. **88:**1–68.
18. **Skerman, V. B. D.** 1967. A guide to the identification of the genera of bacteria, 2nd ed. The Williams & Wilkins Co., Baltimore.
19. **U.S. Department of Health and Human Services.** 1990. Toxicological profile for polycyclic aromatic hydrocarbons. U.S. Department of Health and Human Services, Washington, D.C.